De Novo Design of Non-coordinating Indolones as Potential Inhibitors for Lanosterol 14-α-Demethylase (CYP51)

Rodolfo González-Chávez,[a,b] Roberto Martínez,[c] María Eugenia Torre-Bouscoulet,[b] Marco Gallo,[b] and Marco Martín González-Chávez*[,b]

[a] *Posgrado en Ciencias en Bioprocesos, Universidad Autónoma de San Luis Potosí;* [b] *Facultad de Ciencias Químicas, Universidad Autónoma de San Luis Potosí; Av. Dr. Manuel Nava No. 6. Zona Universitaria, San Luis Potosí, S.L.P. 78210, México: and* [c] *Instituto de Química, Universidad Nacional Autónoma de México; Circuito Exterior de Ciudad Universitaria 04510, México D.F.*

Received December 28, 2012; accepted September 26, 2013

The development of antifungal drugs that inhibit lanosterol 14-α-demethylase (CYP51) *via* non-covalent ligand interactions is a strategy that is gaining importance. A series of novel tetraindol-4-one derivatives with 1- and 2-(2,4-substituted phenyl) side chains were designed and synthesized based on the structure of CYP51 and fluconazole. The antifungal activities of these derivatives against eight human pathogenic filamentous fungi and yeast strains were evaluated *in vitro* by measuring the minimal inhibitory concentrations. Nearly all tested compounds 8a–g displayed activity against *Candida tropicalis*, *Candida guilliermondii* and *Candida parapsilosis* with a minimum inhibitory concentration (MIC) value until 8 $\mu g\,mL^{-1}$, on the other hand compounds 7a–g showed activity against *Aspergillus fumigatus* with a MIC value of 31.25 $\mu g\,mL^{-1}$. A molecular modeling study of the binding interactions between compounds 6, 7d, 8g and the active site of MtCYP51 was conducted based on the computational docking results.

Key words antifungal agent; azole; *Candida* spp.; lanosterol 14-α-demethylase (CYP51) inhibitor; tetrahydroindol-4-one

Opportunistic mycosis caused by *Candida* spp. in immunocompromised patients,[1] pharmaco-resistance due to the modified genetic expression of blank proteins in *C. albicans* and *C. krusei*,[2,3] an increase in the pathogenicity of *C. glabrata* strains,[4] and the limited number of pharmacological therapy options today[5] have together prompted the *de novo* design of antifungal drugs with new mechanisms of inhibition.

The 2001 report by Podust *et al.* of the crystal structure of lanosterol 14-α-demethylase (CYP51) laid the foundations for a new strategic approach to the design of inhibitors against this enzyme.[6–8] The new strategy, which used the same approach employed by azole drugs, relied on imidazole and triazole groups to function as electron-donating pairs and form a coordinating bond with the iron atom of the heme group.[9] Azole drugs tend to suffer from a low selectivity toward the various isoforms of the ubiquitous family of CYPs.[10] With a high affinity toward the heme group, azole drugs form covalent irreversible bonds that translate into a high toxicity.[11] An alternative and promising strategy replaces covalent with electrostatic binding by introducing hydrophobic and bioisosteric groups that interact strongly with hydrophobic residues in the cavities of the CYP51 active site. The challenge, then, is to identify ancillary groups that enhance binding and inhibition without promoting covalent bond formation.

One of the main disadvantages of azole drugs is their strong affinity to the Fe moiety of the hemo group present in CYPs, causing low selectivity to specific isoforms of this group of enzymes, which in turn, could cause toxic effects on the organism; therefore it is very important to design of non-coordinating compounds, such as tetrahydroindol-4-ones.[12] Recent studies indicate that the affinities of pharmacophores to CYP51 did not depend on the coordination of a heterocycle to the heme iron. For example, compounds **1**–**3** are potent inhibitors of CYP51[13–15] and present a high bioisosteric affinity to hydrophobic cavities, forming strong non-covalent interactions including van der Waals, π–π stacking, and hydrogen bonds, see Fig. 1.

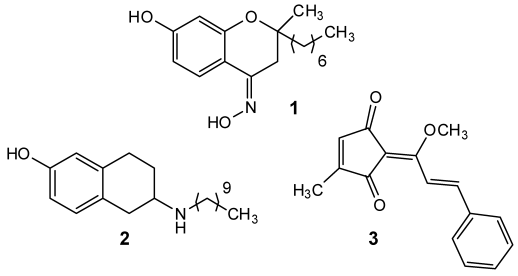

Fig. 1. Non-coordinating Inhibitors of CYP51

Here, we have designed several indolone-type compounds that do not coordinate the heme Fe atom. The design principles were guided by the isosterism observed in molecular fragments of lanosterol **4** and the azoles **5**,[16,17] as directed toward the affinity of the hydrophobic residues (Tyr76, Phe78, Met79 Phe83, Arg96, Phe255, Ala256, His259, Leu321, Ile322, Ile323, Met433 and Val434) in the active site of CYP51.

In this work, we present the synthesis, *in vitro* antifungal evaluation, and molecular modeling of derivatives of tetrahydroindol-4-ones **6**, **7** and **8** (Chart 1).

Relatively few studies have examined the biological activities of indol-4-ones. Such studies have described the cytotoxic activities obtained upon introduction of amino acids,[18] sugars,[19] sulfonamides,[20] or other groups with Lewis base characteristics.[21,22] Martinez *et al.* prepared non-cytotoxic derivatives of the structures **6**, **7** and **8**.[18] All previous studies reported the same observation that the introduction of hydrophobic groups did not yield cytotoxicity, making these deriva-

The authors declare no conflict of interest.

* To whom correspondence should be addressed. e-mail: gcmm@uaslp.mx

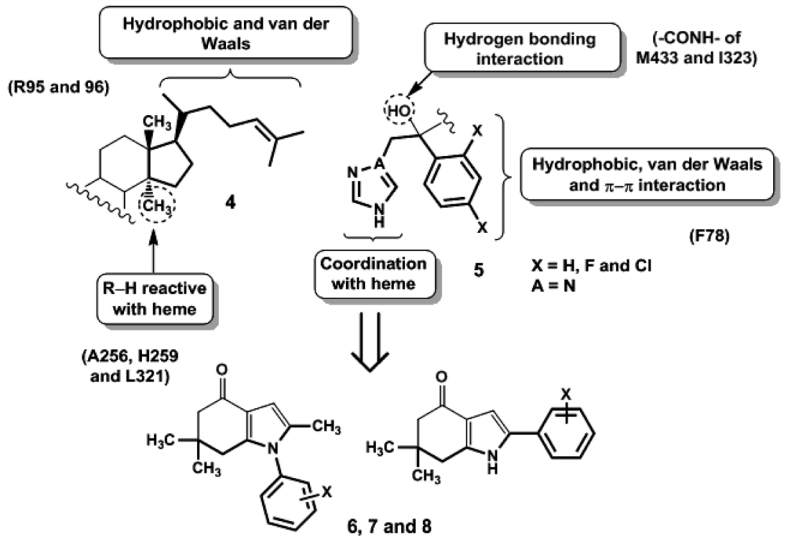

Chart 1. Design of Indol-4-ones from Lanosterol **4** and the Azole Core **5**

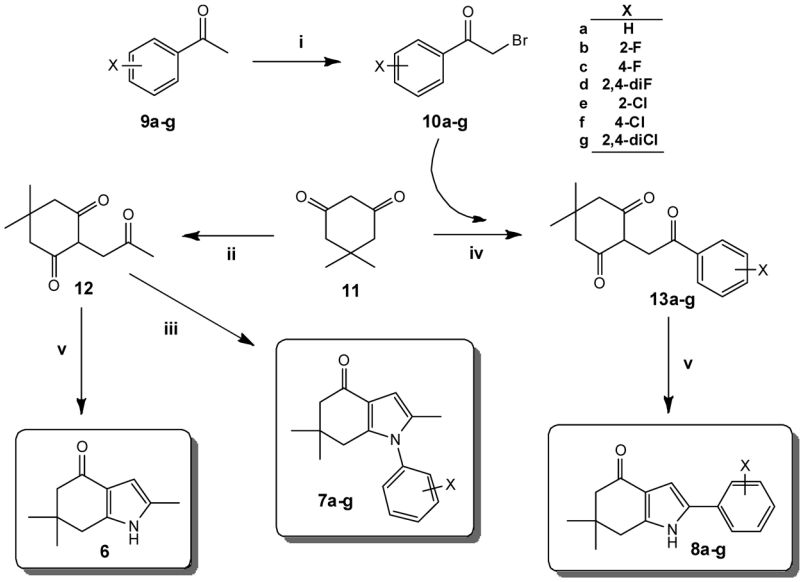

Reaction conditions: i, 1 eq NBS/1.5 eq TsOH·H_2O/ACN/reflux; ii, 1 eq $ClCH_2COCH_3$/1 eq EtONa/EtOH/atm N_2; iii, X-aniline/90°C IR 4 h; iv, 1.8 eq K_2CO_3/CH_2Cl_2/12 h atm N_2; v, NH_4OAc/90°C IR 4 h.

Chart 2

tives excellent candidates for the development of antifungal drugs that inhibit CYP51 in a non-coordinative manner.

Chemistry

The synthesis of compounds **6** and **7a**–**g** began with the preparation of the tricarbonyl compound **12** from the dimedone **11** *via* nucleophilic substitution by chloroacetone in the presence of the base sodium ethoxide under a nitrogen atmosphere. The formation of the pyrrole ring of compound **12** was achieved through the Paal–Knorr reaction in acetic acid in the presence of NH_4OAc to form compound **6** or in the presence of X-anilines to form compounds **7a**–**g**.

For the synthesis of compounds **8a**–**g**, the enols of compounds **10a**–**g** were synthesized from the X-acetophenones **9a**–**g** using *p*-toluenesulfonic acid and *N*-bromosuccinimide (NBS). Nucleophilic substitution of the tricarbonyl compounds **13a**–**g** using K_2CO_3 as a base yielded the dimedone enolate **11**, which was then submitted to nucleophilic substitution in the presence of the bromoacetophenones **10a**–**g**. We then obtained compounds **8a**–**g** *via* the Paal–Knorr reaction using NH_4OAc (Chart 2).

Results and Discussion

The *in vitro* activities of compounds **6**, **7a**–**g**, and **8a**–**g** were evaluated in a growth assay involving several opportunistic pathogenic yeast (*C. albicans*, *C. glabrata*, *C. guilliermondii*, *C. krusei*, and *C. tropicalis*) and fungi (*A. niger* and *A. fumigatus*), as summarized in Table 1. The minimum inhibitory concentration (MIC) values were compared with fluconazole (Flu), itraconazole (Itr) and amphotericin (Amp) as references.

Analysis of the MIC of compounds **6**, **7a**–**g**, and **8a**–**g** revealed that inhibitory activity was present in the lead compound **6** across all *Candida* species (con excepción de *C. parapsilosis*) evaluated over a concentration range of 250–500 $\mu g\,mL^{-1}$ after 24 h incubation. The structural ad-

Table 1. MIC[a] *in Vitro* of **6**, **7a–g** and **8a–g** against *Candida* spp.[b] and *Aspergillus* spp.[c]

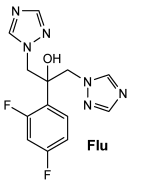

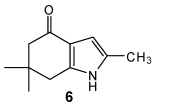

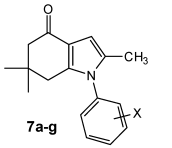

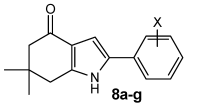

Compound	X	*C. albicans*		*C. glabrata*		*C. krusei*		*C. tropicalis*		*C. guilliermondii*		*C. parapsilosis*		*A. niger*		*A. fumigatus*	
		24 h	48 h	24 h	48 h	24 h	48 h	24 h	48 h	24 h	48 h	24 h	48 h	48 h	72 h	48 h	72 h
6		250	500	500	1000	500	1000	250	1000	250	500	8	62.5	125	250	125	250
7a	H	62.5	500	250	1000	250	1000	125	1000	125	125	8	62.5	62.5	125	62.5	125
7b	2-F	62.5	500	125	1000	250	1000	125	1000	125	125	16	62.5	62.5	62.5	31.25	125
7c	4-F	62.5	500	125	1000	250	1000	125	1000	125	125	16	250	125	250	62.5	250
7d	2,4-diF	125	250	250	1000	125	250	62.5	125	125	125	16	62.5	62.5	125	125	250
7e	2-Cl	125	250	250	1000	125	250	62.5	125	125	125	31.25	31.25	62.5	250	31.25	125
7f	4-Cl	125	250	250	1000	125	250	62.5	125	125	125	16	62	125	>250	125	250
7g	2,4-diCl	125	250	250	1000	125	250	62.5	125	125	125	31.25	250	>250	>250	125	125
8a	H	125	250	125	1000	125	250	62.5	125	62.5	125	16	250	>250	>250	250	250
8b	2-F	125	250	125	250	125	250	62.5	125	62.5	62.5	16	62	>250	>250	250	250
8c	4-F	62.5	250	125	250	62.5	125	31.25	62.5	31.25	62.5	16	62	>250	>250	>250	>250
8d	2,4-diF	62.5	250	125	250	62.5	125	31.25	62.5	31.25	62.5	16	250	>250	>250	>250	>250
8e	2-Cl	62.5	250	125	250	62.5	125	31.25	62.5	31.25	31.25	31.25	250	>250	>250	>250	>250
8f	4-Cl	62.5	250	125	250	62.5	125	31.25	62.5	31.25	31.25	16	62	>250	>250	>250	>250
8g	2,4-diCl	62.5	250	125	250	62.5	125	31.25	31.25	31.25	31.25	31.25	62	>250	>250	>250	>250
Flu[d]		0.25	7.81	2	3.9	8	15.62	0.25	0.98	0.5	0.98	2	4	ND	ND	ND	ND
Itr[e]		0.125	0.125	0.125	0.975	0.125	0.5	0.125	0.25	0.25	0.5	0.125	0.25	1	5	1	4
Amp[f]		0.25	1.95	0.5	0.98	0.5	0.1	0.25	0.1	0.1	0.25	0.25	0.5	0.25	1	0.5	1

a) MIC ($\mu g\,mL^{-1}$) values were determined as described in Experimental. Experiments were performed in triplicate. *b*) *C. albicans* (ATCC 24433), *C. glabrata* (ATCC 66032), *C. krusei* (ATCC 14243), *C. tropicalis* (ATCC 750), *C. guilliermondii* (ATCC 6260) and *C. parapsilosis* (ATCC 22019). *c*) *A. niger* (ATCC 16404) and *A. fumigatus* (ATCC 204305). *d*) Fluconazole (Flu). *e*) Itraconazole. *f*) Amphotericin B (Amp).

dition of a phenyl group to position 1 of the indolones led to an increase in the fungal activity, corresponding to MIC values of 62.5–250 $\mu g\,mL^{-1}$ for the indolones **7a**–**c** in the *C. albicans* assay and an MIC value of 62.5 $\mu g\,mL^{-1}$ for the indolones **7d**–**g** in the *C. tropicalis* assay after 24 h incubation. The change in position of the phenyl group from position 1 to position 2 in the indolones increased the antifungal activity across all *Candida* species tested. The indolones **8c**–**g**, in particular, presented higher activities against *C. tropicalis* and *C. guilliermondii*, with an MIC of 31.25 $\mu g\,mL^{-1}$ after 24 h incubation. The type of halogen and its position on the phenyl ring did not appreciably affect the antifungal activities against the majority of *Candida* species; nevertheless, the greater antifungal activity change was in the indolones **7b**, **7c**, and **7d**, because indolone **7d** included two fluorine atoms and was eight times more active in *C. tropicalis* after 48 h incubation. *C. parapsilosis* showed the highest sensitivity to the indolone-compounds used in this work, compounds **6** and **7a** showed high activity at MIC of 8 $\mu g\,mL^{-1}$ after 24 h incubation. In the case of compounds **7b**–**g** and **8a**–**g** a reduction of the antifungal activity was showed using MICs of 16 and 31.25 respectively, which could be due to the presence of a substituted phenyl group in these compounds. The majority of the indolones yielded MIC values after 48 h incubation that were twice the values after 24 h incubation for all *Candida* strains.

The MIC values for the filamentous fungi used in this work, showed that these species are more sensitive to compounds **6**,**7a**–**f**, contrary to the activity showed for the majority of the *Candida* strains with a MIC between 31.25–250 $\mu g\,mL^{-1}$. It was observed that the halogen and its position in the phenyl ring does not influence in to antifungal activity against *A. niger*. However it was observed that a chlorine or fluorine moeity on the C2 of the phenyl ring improves the activity against *A. Fumigatus* with a MIC of 31.5 $\mu g\,mL^{-1}$.

Molecular Modeling Molecular docking studies were performed using the structure of lanosterol 14-α-demethylase, obtained from *Mycobacterium tuberculosis* (MtCYP51), in complex with fluconazole (Protein Data Bank (PDB) ID. 1EA1) as a template. This structure has been used previously to study and predict ligand–receptor interactions and to rationally design more selective and efficient antifungal compounds.[23] The use of MtCYP51 has been validated in design studies of new azole compounds,[24] mutational maps,[25] and homology models[26] that demonstrated a high degree of similarity between the hydrophobic cavities of the catalytic site of CYP51 from *Candida* spp. and that of MtCYP51.

As the first step, we validated our docking procedure using Glide extra precision (XP)[27,28] by identifying a binding conformation that resembled, as predicted by the Glide XP score, the experimental position from the X-ray crystallography study.

To this end, the fluconazole molecule was removed from the active site of the PDB structure, and the molecule was re-docked in the active site. Our docking procedure produced a structure that agreed well with the experimentally determined docking conformation of fluconazole in the active site, with a root mean square deviation (RMSD) of 1.34 Å. This RMSD value provided support for the validity of our docking procedure.[29] The scores and docking conformations of the indolones were obtained by optimizing the molecular structures using the Gaussian 03 software[30] at the DFT/B3LYP/6-311G** level of theory. The optimization was verified by calculating the vibrational frequencies. The optimized molecules were then docked in the active site of MtCYP51 using Glide XP.

Table 2. Comparison of the Experimentally Determined Activities in *C. tropicalis* and *C. guilliermondii*, and the Glide XP Ecoul and Glide XP Energies, Reported in kcal mol^{-1}

No.	*C. tropicalis*[a]	*C. guilliermondii*[a]	Glide XP ecoul[b]	Glide XP energy[b]
6	1.4105	1.4105	−1.145	−24.013
7a	0.4934	0.4934	0.229	−23.492
7b	0.4607	0.4607	0.955	−23.33
7c	0.4607	0.4607	0.847	−30.404
7d	0.2160	0.4320	1.911	−18.952
7e	0.2172	0.4344	0.544	−28.279
7f	0.2172	0.4344	1.093	−14.524
7g	0.1940	0.3879	0.376	−16.79
8a	0.2612	0.2612	−2.178	−30.45
8b	0.2429	0.2429	−2.839	−34.058
8c	0.1215	0.1215	−1.634	−32.911
8d	0.1135	0.1135	−2.298	−34.388
8e	0.1142	0.1142	−3.738	−33.143
8f	0.1142	0.1142	−1.98	−35.923
8g	0.1014	0.1014	−3.233	−37.858
Flu	0.0008	0.0016	−12.380	−49.401

a) MIC (mmol) values were determined as described in Experimental. *b*) Data (kcal mol^{-1}) generated using Glide 5.6.

The energies obtained from the Glide XP docking study are displayed in Table 2. Shown are the sum of the van der Waals and Coulombic energies, from the Glide XP study, and the Coulombic energy, from the Glide XP ecoul study. Compounds **8a**–**g** gave the minimum Glide XP energies and Glide XP ecoul energies. These compounds also yielded the lowest MIC values against two species of *Candida*. These results suggested that shifting the position of the halophenylic group from N-1 to C-2 resulted in an increase in the antifungal activity. A detailed comparative analysis of the docking of complexes **8g**–MtCYP51 and **7g**–MtCYP51 (Fig. 2) revealed different interactions that played key role in the binding of **8a**–**g** to the active site. The most significant interaction of **8g** involved a hydrogen bond between the oxygen in the ketone group and the Arg96 residue, with a distance of 2.038 Å. One of the methylene groups of the cyclohexanone ring was positioned perpendicular to the porphyrin plane, 4.661 Å from the Fe atom in the heme group, whereas the other methylene group was stabilized by hydrophobic interactions with Ala256.

The 2,4-dichlorophenyl ring was stabilized by face-to-face π–π stacking with Tyr76 and edge-to-face π–π stacking with residue Phe78, located in the upper portion of the ring. The lower portion of the ring was stabilized on one side by Leu321, His259, Met433, and Val435 and on the other side by Ile323 and Leu324.

A docking analysis of complex **7g**–MtCYP51 revealed an adjustment in the orientation of the indolone group to avoid forming a hydrogen bond between the indolone oxygen group and the Arg96 residue. One of the methylene groups in the cyclohexanone ring was positioned perpendicular to the porphyrin plane 3.044 Å from the Fe atom in the heme group, whereas the other methylene was stabilized by hydrophobic interactions with the Thr260 residue. The 2,4-dichlorophenyl ring occupied the same hydrophobic cavity as compound

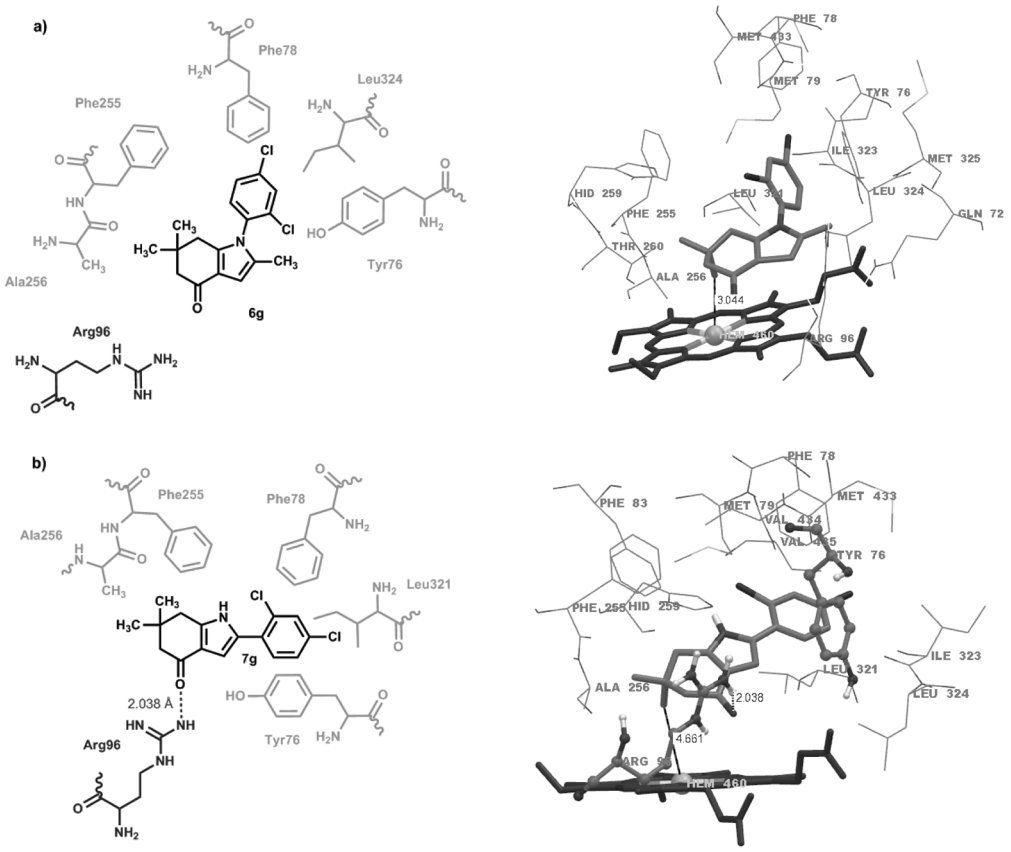

Fig. 2. Predicted Binding Modes and Docking Conformations of the Representative Compounds a) **7g** and b) **8g** in the Active Site of MtCYP51

Atom colors: white (H), gray (C), blue (N), red (O), dark green (Cl), turquoise (Fe) and pink (heme). Amino acid colors: purple (positive polar) and green (hydrophobic). Hydrogen bonds are indicated by dashed lines in red. Hydrogen atoms are omitted for the sake of clarity, except for those involved in bonding interactions. (Color images were converted into gray scale.)

8g, stabilized by π–π face-to-face stacking interactions with residue Tyr76, and the lower portion was stabilized by residue Leu321.

The differences between the interactions present for compounds **8** and **7** are reflected by a decrease in the XP Glide energy and an increase in the antifungal activity of compounds **8a**–**g**. Replacement of the fluorine group to a chlorine group increased contact with the hydrophobic residues Met433 and Val435. This suggested that a change in the antifungal activities *via* regioisomeric changes in the tetrahydroindol-4-ones was related not only to the position of the indolone group, but also to the position of the halogen in the halophenyl ring in the active site of MtCYP51.

The minimum Glide XP energies and Glide XP ecoul energies of indolones and MIC to *Aspergillus* spp. not correlate.

Conclusion

A structure–activity relationship (SAR) analysis was performed to examine the binding modes of molecular fragments of the principal active substrates to the active site of CYP51. The SAR results, in combination with a molecular docking study of select antifungal agents, guided the design, synthesis, and *in vitro* evaluation of a series of derivatives of the substituted tetrahydroindol-4-ones. Some of the newly synthesized compounds were found to be effective against *Candida* spp. Compounds with hydrophobic halophenyl groups at the C-2 position (**8a**–**g**) demonstrated excellent antifungal activities against all yeast strains evaluated. Compounds **8e**–**g** presented a moderate but significant inhibitory effect over *C. tropicalis* and *C. guilliermondii*. These results indicated that a change in the position of the halophenyl regioisomers from N-1 to C-2 increased the antifungal activity. The molecular docking study provided a better understanding of the key interactions between the drugs and the active site of MtCYP51. *C. parapsilosis* was the most sensitive yeast strain to the indolone-compounds used in this work, showing compounds **6** and **7a** the highest activity. In the case of filamentous fungi strains, *A. fumigatus* showed the highest sensitivity to the compounds **7b** and **7e**. Recent advances in SAR studies of fragments of tetrahydroindol-4-ones are helpful toward elucidating new non-coordinating antifungal compounds with broad activity spectra and high potency. Further structural optimization studies, such as estereoelectronic effects due to electron-releasing and electron-withdrawing groups and bioisosteric effects in indolones are in progress.

Experimental

General General methods: All reagents and solvents were reagent-grade and were used as received from Sigma-Aldrich Co. (St. Louis, MO, U.S.A.). Flash chromatography was performed using E. Merck Kieselgel 60 silica gel (230–400 mesh). Reported melting points are uncorrected. The FT-IR were recorded on a Thermo Nicolet Nexus 470 FT-IR as thin films on a KBr disk (for solids) and as a germanium ATR crystal (for liquids). ^{1}H- and ^{13}C-NMR were obtained on an Eclipse Jeol (operated at 300, 75 MHz, respectively)

and a Varian–Gemini (operating at 200 MHz and 50 MHz, respectively). Chemical shifts are expressed as δ values (ppm) relative to tetramethylsilane (TMS) as an internal standard (s=singlet, d=doublet, t=triplet, q=quadruplet, sext=sextuplet, m=multiplet and br=broad). Coupling constants (*J*) are given in Hertz (Hz). All mass spectra (MS) were recorded on a Jeol AX505HA mass spectrometer. Elemental analyses were performed on a CE-440 Exeter Analytical Inc. The purity of compounds **6**, **7a**–**g** and **8a**–**g** (>97%) was analyzed using an Agilent Technology GC 6890N coupled with a MS 5973N mass spectrometer operated at 70 eV and equipped with a DB-5HT capillary column (15 m, 0.25 i.d.) with a (5%-phenyl)-methylpolysiloxane (0.10 μm film). Helium was used as the carrier gas at a flow rate of 1 mL/min. The injector and MS transfer line temperatures were set at 300°C. Diluted samples (1 : 10 v/v, in acetone) 2.0 μL in volume were manually injected. After sample injection, the initial temperature in the oven (100°C) was held constant for 2 min, then increased to 300°C (at a rate of 20°C/min). This temperature was then maintained for 3 min. After a delay of 1.8 min to permit passage of the solvent, the mass spectra were scanned from 15 to 800 *m/z*.

5,5-Dimethyl-2-(2-oxopropyl)cyclohexane-1,3-dione (12) A mixture of 14 mmol sodium ethoxide, 2 g (14 mmol) 5,5-dimethylcyclohexane-1,3-dione and 1.33 mL (14 mmol) chloroacetone in 20 mL ethanol was heated under reflux for 30 min and then cooled. The sodium chloride that formed was removed by filtration, and the filtrate was concentrated *in vacuo*. The residual syrup was dissolved in a mixture of chloroform (20 mL) and 10% sodium hydroxide (20 mL). The aqueous phase was separated and re-extracted with chloroform (20 mL). The aqueous phase was cooled in an ice bath, made acidic with the addition of hydrochloric acid, and extracted with chloroform (3×20 mL). The combined organic extracts were dried with anhydrous sodium sulfate and filtered, and the filtrate was evaporated *in vacuo* to dryness. Recrystallization of the crude product from acetone gave compound **12** as colorless crystals (2.2 g, 80%): *Rf*=0.22 (hexane–AcOEt, 70 : 30); mp 133–135°C. ^{1}H-NMR (200 MHz, DMSO-d_6) δ: 0.99 (s, 6H), 1.98 (s, 3H), 2.22 (s, 4H), 3.16 (s, 1H), 3.33 (s, 1H), 10.62 (s, 1H). MS (electron ionization (EI)): *m/z* (%): 196 (M^+, 51), 154 (89), 125 (24), 98 (100), 55 (45). IR (KBr) $\tilde{\nu}$: 2962, 2931, 1720, 1645, 1155, 1064 cm^{-1}.

General Procedure for the Synthesis of 2-(2-(X-Phenyl)-2-oxoethyl)-5,5-dimethylcyclohexane-1,3-dione, 13a–g A slurry of dimedone **11** (1 eq), bromoketone **10a-g** (1 eq), and anhydrous K_2CO_3 (1.8 eq) in chloroform was stirred at room temperature for 12 h. The mixture was then filtered. The insoluble salts were dissolved in water, and the filtered solution was made acidic by the addition of concentrated HCl. The precipitate was filtered off, washed with water, and crystallized from acetone.

5,5-Dimethyl-2-(2-oxo-2-phenylethyl)cyclohexane-1,3-dione (**13a**): The title compound was obtained as a white powder (1.3 g, 39.5%): *Rf*=0.47 (hexane–AcOEt, 70 : 30); mp 136–138°C. ^{1}H-NMR (200 MHz, DMSO-d_6) δ: 0.97 (s, 6H), 2.10 (s, 4H), 3.79 (s, 2H), 7.44–7.63 (m, 3H), 7.90–7.95 (m, 2H), 10.96 (s, 1H). MS (EI): *m/z* (%): 258 (M^+, 11), 140 (30), 105 (34), 83 (100), 56 (55). IR (KBr) $\tilde{\nu}$: 2960, 2869, 2680, 2630, 2576, 2532, 1617, 1577, 1519, 1471, 1349, 1305, 1226, 1145 cm^{-1}.

2-[2-(2-Fluorophenyl)-2-oxoethyl]-5,5-dimethylcyclohexane-1,3-dione (**13b**): The title compound was obtained as a white powder (0.9 g, 29%): *Rf*=0.42 (hexane–AcOEt, 70 : 30); mp 156°C. ^{1}H-NMR (200 MHz, DMSO-d_6) δ: 0.97 (s, 6H), 2.1 (s, 2H), 2.18 (s, 2H), 3.70 (d, 2H, *J*=2.2 Hz), 7.24–7.35 (m, 2H), 7.54–7.65 (m, 1H), 7.71 (ddd, 1H, *J*=8.8, 8.5, 0.8 Hz) 10.67 (s, 1H). ^{13}C-NMR (50 MHz, DMSO-d_6) δ: 27.8, 31.7, 35.6, 36.4, 38.2, 102.4, 107.8, 116.6, 124.5, 126.0, 130.0, 134.2, 158.0, 163.0, 196.0. MS (EI): *m/z* (%): 276 (M^+, 56), 153 (30), 123 (100), 97 (25), 83 (21), 55 (12). IR (KBr): $\tilde{\nu}$: 3127, 2958, 2892, 1683, 1608, 1247, 1195, 765 cm^{-1}.

2-[2-(4-Fluorophenyl)-2-oxoethyl]-5,5-dimethylcyclohexane-1,3-dione (**13c**): The title compound was obtained as a yellow-orange powder (1.5 g, 68%): *Rf*=0.47 (hexane–AcOEt, 70 : 30); mp 96°C. ^{1}H-NMR (200 MHz, DMSO-d_6) δ: 0.97 (s, 6H), 2.1 (s, 2H), 2.38 (s, 2H), 3.77 (s, 2H), 7.31 (dd, 2H, *J*=8.8, 9 Hz), 8.01 (dd, 2H, *J*=9 Hz), 10.99 (s, 1H). MS (EI): *m/z* (%): 276 (M^+, 26), 162 (14), 123 (100), 95 (14), 83 (29), 55 (13). IR (KBr) $\tilde{\nu}$: 3081, 2960, 2871, 2628, 2578, 1691, 1602, 1515, 1469, 1349, 1307, 1228, 1147, 1039, 998, 831 cm^{-1}.

2-[2-(2,4-Difluorophenyl)-2-oxoethyl]-5,5-dimethylcyclohexane-1,3-dione (**13d**): The title compound was obtained as a yellow powder (2.1 g, 73%): *Rf*=0.47 (hexane–AcOEt, 70 : 30); mp 138°C. ^{1}H-NMR (200 MHz, DMSO-d_6) δ: 0.97 (s, 6H), 2.22 (s, 4H), 3.68 (d, 2H, *J*=2.4 Hz), 7.18 (ddd, 1H, *J*=7.2, 9.6, 0.8 Hz), 7.37 (ddd, 1H, *J*=11.45, 9.3, 2.6 Hz), 7.81 (ddd, 1H, *J*=16, 7.6, 1.8 Hz), 10.61 (s, 1H). ^{13}C-NMR (50 MHz, DMSO-d_6) δ: 27.8, 31.8, 36.3, 44.6, 104.9, 107.7, 112.1, 122.7, 132.2, 158.8, 1162.0, 163.9, 167.03, 172.9, 194.7. MS (EI): *m/z* (%): 294 (M^+, 46), 153 (30), 141 (100), 97 (24), 83 (14), 55 (8). IR (KBr) $\tilde{\nu}$: 3077, 2964, 2892, 2657, 1695, 1608, 1577, 1243, 1199, 1147, 1099, 1039 cm^{-1}.

2-[2-(2-Chlorophenyl)-2-oxoethyl]-5,5-dimethylcyclohexane-1,3-dione (**13e**): The title compound was obtained as a white powder (0.7 g, 20%): *Rf*=0.32 (hexane–AcOEt, 70 : 30); mp 142°C. ^{1}H-NMR (200 MHz, DMSO-d_6) δ: 0.97 (s, 6H), 2.1 (s, 4H), 5.70 (s, 2H), 7.6 (m, 4H) 10.98 (s, 1H). ^{13}C-NMR (50 MHz, DMSO-d_6) δ: 27.9, 31.1, 32.1, 53.2, 63.3, 102.4, 126.7, 130.0, 131.4, 138.5, 200.1, 204.7. MS (EI): *m/z* (%): 292 (M^+, 1), 140 (57), 112 (23), 83 (100), 56 (49) 55 (35). IR (KBr) $\tilde{\nu}$: 2960, 2869, 2680, 2576, 2530, 1907, 1617, 1581, 1519, 1471, 1349, 1305, 1228, 1145 cm^{-1}.

2-[2-(4-Chlorophenyl)-2-oxoethyl]-5,5-dimethylcyclohexane-1,3-dione (**13f**): The title compound was obtained as a white powder (0.9 g, 47%): *Rf*=0.5 (hexane–AcOEt, 70 : 30); mp 164°C. ^{1}H-NMR (200 MHz, DMSO-d_6) δ: 0,99 (s, 6H), 2,23 (s, 4H), 3,77 (s, 2H), 7,55 (dd, 2H, *J*=8.6, 1.6 Hz), 7,94 (dd, 2H, *J*=8.6, 1.6 Hz) and 10,65 (s, 1H). MS (EI): *m/z* (%): 292 (M^+, 51), 153 (14), 139 (100), 111 (16), 97 (16), 55 (5). IR (KBr) $\tilde{\nu}$: 3162, 2956, 2917, 2871, 1685, 1600, 1411, 1378, 1321, 1251, 1193, 1145, 1039, 993, 813, 777 cm^{-1}.

2-[2-(2,4-Chlorophenyl)-2-oxoethyl]-5,5-dimethylcyclohexane-1,3-dione (**13g**): The title compound was obtained as a white powder (0.4 g, 10%): *Rf*=0.27 (hexane–AcOEt, 70 : 30); mp 140°C. ^{1}H-NMR (200 MHz, DMSO-d_6) δ: 0.97 (s, 6H), 2.10 (s, 4H), 5.17 (s, 2H), 7.48 (dd, 1H, *J*=8.4, 1.8 Hz), 7.58 (d, 1H, *J*=8.4 Hz), 7.66 (d, 1H, *J*=1.8 Hz), 10.96 (s, 1H). ^{13}C-NMR (50 MHz, DMSO-d_6) δ: 27.9, 32.1, 46.1, 102.4. MS (EI): *m/z* (%): 326 (M^+, 9), 173 (42), 140 (79), 112 (32), 83 (100) 56 (74), 55(63). IR (KBr) $\tilde{\nu}$: 2960, 2871, 2630, 2576, 2532, 1700, 1617, 1577, 1521, 1471, 1349, 1305, 1251, 1226, 1145 cm^{-1}.

General Procedure for the Synthesis of 1-(X-Phenyl)-2,6,6-

trimethyl-6,7-dihydro-1*H*-indol-4(5*H*)-one (6, 7a–g, 8a–g) To a vigorously stirred suspension of tricarbonyl compounds **13a**–**g** (3.88 mmol) in AcOH (5 mL) *R*-aniline was added to **7a**–**g** or NH_4OAc to yield **6** and **8a**–**g** (3.88 mmol). The resulting slurry was heated to 90°C for 4 h using an IR lamp. The reaction mixture was then allowed to cool to room temperature and poured into ice water (10 mL). The solid was filtered and washed with cooled water. The crude mixture was purified by column chromatography on silica gel using a gradient of 30–50% AcOEt in hexane as the eluent. Evaporation of the collected fractions gave indolones **6**, **7a**–**g** and **8a**–**g**. The spectral data for the tetrahydroindol-4-ones **6**, **7a**, **7c**, **7f**, **8a**, **8c**, and **8f** were in agreement with the reported data.[31] Spectral data for the unknown tetrahydroindol-4-ones **7b**, **7d**, **7e**, **7g**, **8b**, **8d**, **8e** and **8g** are described below.

2,6,6-Trimethyl-6,7-dihydro-1*H*-indol-4(5*H*)-one (**6**): The title compound was obtained as a yellow powder (1.2 g, 72%): *Rf*=0.38 (hexane–AcOEt, 70 : 30); mp 184°C; ^{1}H-NMR (200 MHz, DMSO-d_6) δ: 0.99 (s, 6H), 2.11 (s, 3H), 2.13 (s, 2H), 2.55 (s, 2H), 5.88 (q, 1H, *J*=2.1, 1 Hz), 11.02 (s, 1H). MS (EI): *m/z* (%): 177 (M^+, 65), 121 (92), 93 (100), 66 (7), 42 (13). IR (KBr) $\tilde{\nu}$: 3243, 3170, 2954, 2921, 1629, 1482, 1128, 808 cm^{-1}. GC-MS purity=99.8%; t_R=4.0 min.

2,6,6-Trimethyl-1-phenyl-6,7-dihydro-1*H*-indol-4(5*H*)-one (**7a**): The title compound was obtained as a colorless crystals (0.6 g, 67%): *Rf*=0.68 (hexane–AcOEt, 70 : 30); mp 141°C. ^{1}H-NMR (200 MHz, DMSO-d_6) δ: 0.96 (s, 6H), 1.98 (s, 3H), 2.16 (s, 2H), 2.38 (s, 2H), 6.19 (q, 1H, *J*=1.2, 0.4 Hz), 7.32–7.37 (m, 2H), 7.45–7.60 (m, 3H). MS (EI): *m/z* (%): 253 (M^+, 79), 197 (94), 169 (100), 168 (52), 118 (31), 77 (35). IR (KBr) $\tilde{\nu}$: 3048, 2954, 2925, 2867, 1652, 1529, 1463, 1436, 1403, 1274, 1203, 1120, 1076, 788, 767, 701 cm^{-1}. GC-MS purity=99.9%; t_R=7.4 min.

1-(2-Fluorophenyl)-2,6,6-trimethyl-6,7-dihydro-1*H*-indol-4(5*H*)-one (**7b**): The title compound was obtained as a yellow-orange crystals (0.4 g, 55%): *Rf*=0.68 (hexane–AcOEt, 70 : 30); mp 137°C. ^{1}H-NMR (200 MHz, DMSO-d_6) δ: 0.97 (d, 6H), 1.95 (s, 3H), 2.23 (s, 2H), 2.32 (q, 2H), 6.22 (d, 1H, *J*=1 Hz), 7.37 (dd, 1H, *J*=7.9, 1.8 Hz), 7.41 (dd, 1H, *J*=6.9, 1.6 Hz), 7.52 (dd, 1H, *J*=9.9, 1.8 Hz), 7.57–7.65 (m, 1H). ^{13}C-NMR (50 MHz, DMSO-d_6) δ: 11.7, 27.9, 35.2, 51.5, 103.0, 116.8, 118.6, 123.9, 125.5, 130.2, 131.1, 131.3, 143.3, 154.6, 159.5, 192.0. MS (EI): *m/z* (%): 271 (M^+, 82), 215 (75), 187 (100), 167 (4), 136 (52), 95 (11), 75 (6), 41 (4). IR (KBr) $\tilde{\nu}$: 3046, 2954, 2904, 2869, 1654, 1508, 1463 cm^{-1}. *Anal.* Calcd for $C_{17}H_{18}FNO$: C, 75.25; H, 6.69; N, 5.16. Found: C, 75.48; H, 6.31; N, 5.05. GC-MS purity=99.9%; t_R=7.3 min.

1-(4-Fluorophenyl)-2,6,6-trimethyl-6,7-dihydro-1*H*-indol-4(5*H*)-one (**7c**): The title compound was obtained as a colorless crystals (0.8 g, 59%): *Rf*=0.68 (hexane–AcOEt, 70 : 30); mp 155–158°C. ^{1}H-NMR (200 MHz, DMSO-d_6) δ: 0.96 (s, 6H), 1.95 (d, 3H), 2.21 (s, 2H), 2.38 (s, 2H), 6.19 (d, 1H, *J*=1 Hz), 7.33–7.47 (m, 4H). MS (EI): *m/z* (%): 271 (M^+, 90), 215 (100), 187 (95), 172 (9), 136 (31), 95 (24). IR (KBr) $\tilde{\nu}$: 3066, 2956, 2904, 2871, 1648, 1513, 1465, 1413, 1224, 1120, 1045, 863, 794 cm^{-1}. GC-MS purity=99.9%; t_R=7.3 min.

1-(2,4-Difluorophenyl)-2,6,6-trimethyl-6,7-dihydro-1*H*-indol-4(5*H*)-one (**7d**): The title compound was obtained as a colorless crystals (1.1 g, 68%): *Rf*=0.68 (hexane–AcOEt, 70 : 30); mp 137°C. ^{1}H-NMR (200 MHz, DMSO-d_6) δ: 0.97 (d, 6H), 1.95 (s, 3H), 2.23 (s, 2H), 2.32 (q, 2H), 6.21 (q, 1H, *J*=1, 0.4 Hz), 7.28–7.35 (m, 1H), 7.54–7.66 (m, 2H). ^{13}C-NMR (50 MHz, DMSO-d_6) δ: 11.9, 27.8, 35.2, 51.5, 103.0, 105.4, 112.6, 118.7, 120.5, 131.3, 131.6, 143.5, 154.9, 159.8, 164.6, 192.0. MS (EI): *m/z* (%): 289 (M^+, 89), 233 (94), 205 (100), 154 (54), 113 (9). IR (KBr) $\tilde{\nu}$: 3073, 2956, 2931, 2869, 1648, 1608, 1517, 1465, 1436, 1272, 1201, 1145, 1105, 962, 860 cm^{-1}. *Anal.* Calcd for $C_{17}H_{17}F_2NO$: C, 70.57; H, 5.92; N, 4.84. Found: C, 70.69; H, 6.09; N, 4.98. GC-MS purity=99.2%; t_R=7.0 min.

1-(2-Chlorophenyl)-6,7-dihidro-2,6,6-trimetil-1*H*-indol-4(5*H*)-one (**7e**): The title compound was obtained as a colorless crystals (0.8 g, 57%): *Rf*=0.63 (hexane–AcOEt, 70 : 30); mp 121°C. ^{1}H-NMR (200 MHz, DMSO-d_6) δ: 0.97 (d, 6H), 1.88 (d, 3H), 2.24 (q, 4H), 6.21 (d, 1H, *J*=1.2 Hz), 7.47–7.63 (m, 3H), 7.69–7.78 (m, 1H). ^{13}C-NMR (50 MHz, DMSO-d_6) δ: 11.9, 27.8, 35.2, 51.5, 103.0, 105.4, 112.6, 118.7, 120.5, 131.3, 131.6, 143.5, 154.9, 159.8, 164.6, 192.0. MS (EI): *m/z* (%): 287 (M^+, 89), 233 (94), 205 (100), 154 (54), 113 (9). IR (KBr) $\tilde{\nu}$: 3073, 2956, 2931, 2869, 1648, 1608, 1517, 1465, 1436, 1272, 1201, 1145, 1105, 962, 860 cm^{-1}. *Anal.* Calcd for $C_{17}H_{18}ClNO$: C, 70.95; H, 6.30; N, 4.87. Found: C, 70.83; H, 6.15; N, 4.70. GC-MS purity=99.9%; t_R=7.9 min.

1-(4-Chlorophenyl)-2,6,6-trimethyl-6,7-dihydro-1*H*-indol-4(5*H*)-one (**7f**): The title compound was obtained as a colorless crystals (0.9 g, 53,5%): *Rf*=0.65 (hexane–AcOEt, 70 : 30), mp 174°C. ^{1}H-NMR (200 MHz, DMSO-d_6) δ: 0.96 (s, 6H), 2.00 (d, 3H), 2.21 (s, 2H), 2.39 (s, 2H), 6.20 (d, 1H, *J*=1 Hz), 7.40 (dd, 2H, *J*=8.8 Hz), 7.61 (dd, 2H, *J*=8.8 Hz). MS (EI): *m/z* (%): 287 (M^+, 86), 231 (100), 203 (47), 168 (93), 152 (23), 111 (7). IR (KBr) $\tilde{\nu}$: 3060, 2956, 2933, 2869, 1648, 1496, 1465, 1436, 1407, 1272, 1228, 1203, 1087, 863, 790, 619 cm^{-1}. GC-MS purity=99.9%; t_R=8.2 min.

1-(2,4-Dichlorophenyl)-2,6,6-trimethyl-6,7-dihydro-1*H*-indol-4(5*H*)-one (**7g**): The title compound was obtained as a yellow crystals (0.6 g, 30%): *Rf*=0.68 (hexane–AcOEt, 70 : 30); mp 176°C. ^{1}H-NMR (200 MHz, DMSO-d_6) δ: 0.97 (d, 6H), 1.89 (d, 3H), 2.49 (q, 4H), 6.21 (d, 1H, *J*=1 Hz), 7.57 (dd, 1H, *J*=8.4, 0.4 Hz), 7.65 (dd, 1H, *J*=8.5, 2.2 Hz), 7.96 (d, 1H, *J*=2 Hz). ^{13}C-NMR (50 MHz, DMSO-d_6) δ: 11.7, 27.4, 28.5, 35.2, 51.6, 102.9, 118.6, 128.8, 129.9, 130.8, 131.8, 133.1, 134.9, 143.1, 191.9. MS (EI): *m/z* (%): 321 (M^+, 81), 265 (100), 237 (46), 202 (71), 145 (8), 109 (5). IR (KBr) $\tilde{\nu}$: 3073, 3035, 2954, 2919, 2867, 1648, 1531, 1490, 1463, 1407, 1280, 1201, 1101, 1072, 1000, 863, 802 cm^{-1}. *Anal.* Calcd for $C_{17}H_{17}Cl_2NO$: C, 63.37; H, 5.32; N, 4.35. Found: C, 63.05; H, 5.34; N, 4.82. GC-MS purity=99.0%; t_R=8.5 min.

6,6-Dimethyl-2-phenyl-6,7-dihydro-1*H*-indol-4(5*H*)-one (**8a**): The title compound was obtained as a white powder (0.2 g, 88%): *Rf*=0.51 (hexane–AcOEt, 70 : 30), mp 227°C. ^{1}H-NMR (200 MHz, DMSO-d_6) δ: 1.04(s, 6H), 2.23 (s, 2H), 2.70 (s, 2H), 6.70 (d, 1H, *J*=2.4 Hz), 7.19 (dd, 1H, *J*=7.3, 7.2 Hz), 7.36 (dd, 2H, *J*=7.5, 7.2 Hz), 7.64 (dd, 2H, *J*=7.9, 1.4 Hz), 11.71 (s, 1H). MS (EI): *m/z* (%): 239 (M^+, 239), 183 (78), 155 (100), 128 (9), 104 (24), 77 (8). IR (KBr) $\tilde{\nu}$: 3513, 3338, 3224, 2964, 2929, 1608, 1488, 1228, 1143, 823, 757, 692, 626 cm^{-1}. GC-MS purity=99.7%; t_R=8.5 min.

2-(2-Fluorophenyl)-6,6-dimethyl-6,7-dihydro-1*H*-indol-4(5*H*)-one (**8b**): The title compound was obtained as a white powder (0.3 g, 73%): *Rf*=0.54 (hexane–AcOEt, 70 : 30); mp 229°C. ^{1}H-NMR (300 MHz, DMSO-d_6) δ: 1.04 (s, 6H), 2.24 (s, 2H), 2.72 (s, 2H), 6.69 (t, 1H, *J*=3 Hz), 7.21–7.29 (m, 3H), 7.68–7.76 (m, 1H), 11.70 (s, 1H). ^{13}C-NMR (75 MHz, DMSO-

d_6) δ: 28.1, 35.5, 51.7, 105.2, 116.2, 119.5, 119.7, 124.7, 126.0, 127.9, 143.9, 156.5, 159.8, 192.1. MS (EI) *m/z* (%): 257 (M^+, 85), 201 (54), 173 (100), 146 (9), 122 (25), 102 (7), 75 (2), 51 (2). IR (KBr) $\tilde{\nu}$: 3286, 3166, 2954, 2919, 1629, 1569, 1492, 1218, 1168, 1139, 819, 755 cm^{-1}. *Anal.* Calcd for $C_{16}H_{16}FNO$: C, 74.69; H, 6.27; N, 5.44. Found: C, 74.01; H, 6.34; N, 5.44. GC-MS purity=97.9%; t_R=8.0 min.

2-(4-Fluorophenyl)-6,6-dimethyl-6,7-dihydro-1*H*-indol-4(5*H*)-one (**8c**): The title compound was obtained as a white powder (0.25 g, 44%): *Rf*=0.49 (hexane–AcOEt, 70 : 30); mp 242°C. ^{1}H-NMR (200 MHz, DMSO-d_6) δ: 1.04 (s, 6H), 2.22 (s, 2H), 2.69 (s, 2H), 6.67 (d, 1H, *J*=2.6 Hz), 7.20 (dd, 2H, *J*=8.9, 8.8 Hz), 7.64–7.71 (m, 2H), 11.70 (s, 1H). MS (EI) *m/z* (%): 257 (M^+, 88), 201 (68), 173 (100), 122 (28), 91 (15). IR (KBr) $\tilde{\nu}$: 3253, 3153, 3060, 2958, 2929, 2869, 1625, 1577, 1527, 1488, 1409, 1230, 1160, 1141, 829, 794 cm^{-1}. GC-MS purity=99.3%; t_R=8.7 min.

2-(2,4-Difluorophenyl)-6,6-dimethyl-6,7-dihydro-1*H*-indol-4(5*H*)-one (**8d**): The title compound was obtained as a white powder (0.4 g, 60%): *Rf*=0.56 (hexane–AcOEt, 70 : 30); mp 247°C. ^{1}H-NMR (300 MHz, DMSO-d_6) δ: 1.04 (s, 6H), 2.23 (s, 2H), 2.71 (s, 2H), 6.64 (t, 1H, *J*=2.8 Hz), 7.16 (ddd, 1H, *J*=7.5, 9.5, 2.2 Hz), 7.33 (ddd, 1H, *J*=9.2, 11.7, 2.6 Hz), 7.74 (dd, 1H, *J*=7.7, 2.6 Hz) 11.71 (s, 1H). ^{13}C-NMR (75 MHz, DMSO-d_6) δ: 28.1, 35.5, 51.7, 104.3, 104.7, 104.9, 111.9, 116.6, 119.4, 125.3, 127.8, 143.9, 156.5, 158.9, 159.8, 162.2, 192.1. MS (EI) *m/z* (%): 275 (M^+, 65), 219 (49), 191 (100), 164 (9), 140 (27), 120 (7). IR (KBr) $\tilde{\nu}$: 3282, 3170, 2958, 2927, 2871, 1621, 1577, 1525, 1490, 1459, 1409, 1288, 1241, 1135, 971, 929, 850, 815 cm^{-1}. *Anal.* Calcd for $C_{16}H_{15}F_2NO$: C, 69.81; H, 5.49; N, 5.09. Found: C, 69.13; H, 5.56; N, 5.06. GC-MS purity=97.6%; t_R=8.1 min.

2-(2-Chlorophenyl)-6,6-dimethyl-6,7-dihydro-1*H*-indol-4(5*H*)-one (**8e**): The title compound was obtained as a white powder (0.5 g, 48%) : *Rf*=0.60 (hexane–AcOEt, 70 : 30); mp 225°C. ^{1}H-NMR (300 MHz, DMSO-d_6) δ: 1.05 (s, 6H), 2.24 (s, 2H), 2.71 (s, 2H), 6.72 (d, 1H, *J*=2.6 Hz), 7.28 (ddd, 1H, *J*=6.6, 8.3, 1.8 Hz), 7.38 (ddd, 1H, *J*=7.5, 8.2, 1.6 Hz), 7.52 (dd, 1H, *J*=7.2, 1.6 Hz), 7.58 (dd, 1H, *J*=7.7, 1.6 Hz), 11.6 (s, 1H). ^{13}C-NMR (75 MHz, DMSO-d_6) δ: 28.1, 35.2, 35.8, 51.7, 105.9, 119.1, 127.3, 128.2, 128.7, 129.3, 130.1, 130.5, 143.5, 192.2. MS (EI) *m/z* (%): 273 (M^+, 70), 217 (69), 189 (69), 138 (19), 69 (57), 28 (100). IR (KBr) $\tilde{\nu}$: 3224, 3147, 3060, 2960, 2925, 2892, 1641, 1488, 1367, 1220, 1164, 1124, 1079, 939, 752, 723 cm^{-1}. *Anal.* Calcd for $C_{16}H_{16}ClNO$: C, 70.20; H, 5.89; N, 5.12. Found: C, 69.37; H, 5.98; N, 5.03. GC-MS purity=97.9%; t_R=8.8 min.

2-(4-Chlorophenyl)-6,6-dimethyl-6,7-dihydro-1*H*-indol-4(5*H*)-one (**8f**): The title compound was obtained as a white powder (0.7 g, 48%): *Rf*=0.53 (hexane–AcOEt, 70 : 30); mp 225°C. ^{1}H-NMR (300 MHz, DMSO-d_6) δ: 1.04 (s, 6H), 2.22 (s, 2H), 2.69 (s, 2H), 6.75 (d, 1H, *J*=1.1 Hz), 7.41 (dd, 2H, *J*=8.6 Hz), 7.67 (dd, 2H, *J*=8.6 Hz), 11.77 (s, 1H). MS (EI) *m/z* (%): 273 (M^+, 30), 217 (24), 189 (30), 139 (100), 111 (13), 97 (12), 69 (8), 28 (11). IR (KBr) $\tilde{\nu}$: 3241, 2956, 2927, 2867, 1625, 1486, 1405, 1222, 1139, 1091, 1033, 933, 819, 794 cm^{-1}. GC-MS purity=99.0%; t_R=9.4 min.

2-(2,4-Dichlorophenyl)-6,6-dimethyl-6,7-dihydro-1*H*-indol-4(5*H*)-one (**8g**): The title compound was obtained as a white powder (0.2 g, 89%): *Rf*=0.60 (hexane–AcOEt, 70 : 30); mp 290°C. ^{1}H-NMR (300 MHz, DMSO-d_6) δ: 1.04 (s, 6H), 2.24 (s, 2H), 2.70 (s, 2H), 6.76 (d, 1H, *J*=4.6 Hz), 7.48 (dd, 1H, *J*=8.6, 2 Hz), 7.60 (d, 1H, *J*=8.6 Hz), 7.68 (d, 1H, *J*=2.2 Hz), 11.74 (s, 1H). ^{13}C-NMR (75 MHz, DMSO-d_6) δ: 28.1, 35.2, 35.8, 51.7, 106.4, 119.2, 127.5, 127.6, 129.4, 129.9, 130.3, 130.8, 131.6, 143.8, 192.2. MS (EI) *m/z* (%) 307 (M^+, 100), 251 (86), 223 (77), 172 (19), 136 (5), 69 (3), 28 (15). IR (KBr) $\tilde{\nu}$: 3251, 3154, 2958, 2929, 2869, 1631, 1490, 1461, 1382, 1220, 1137, 1105, 1076, 808 cm^{-1}. *Anal.* Calcd for $C_{16}H_{15}Cl_2NO$: C, 60.35; H, 4.91; N, 4.54. Found: C, 62.95; H, 5.14; N, 4.53. GC-MS purity=97.8%; t_R=9.5 min.

Antifungal Activity The title compounds **6**, **7a**–**g**, and **8a**–**g** were evaluated for their *in vitro* antifungal activity in comparison with the commercial antifungal fluconazole, itraconazole and amphotericin. The activities were measured in terms of the minimal inhibitory concentrations (MIC) using the serial dilution method in 96-well microtest plates. Test fungal strains were obtained from the *Candida albicans* ATCC 24433, *C. glabrata* ATCC 66032, *C. guilliermondii* ATCC 6260, *C. krusei* ATCC 14243, *C. tropicalis* ATCC 750, *C. parapsilosis* ATCC 22019, *Aspergillus niger* ATCC 16404, *A. fumigatus* ATCC 204305. The MIC determination was performed according to method M27-A3 to yeast and M38-A to filamentous fungi as outlined in the Clinical and Laboratory Standards Institute (CLSI) recommendations using RPMI 1640 (Sigma) buffered with 0.165 M *N*-(2-hydroxyethyl)-piperazine-*N*′-2-ethanesulfonic acid (HEPES) (Sigma) as the test medium. MIC values were defined as the concentrations that inhibited growth of *Candida* spp. and *Aspergillus* spp. by 50% relative to the control, as recommended by the M27-A3 and M38-A guidelines.[32,33] Test compounds were dissolved in EtOH and serially diluted in growth medium. The yeast cells were incubated at 37°C. Growth MIC was determined at 24–48 h for *Candida* spp. and 48–72 h for *Aspergillus* spp.

Molecular Modeling Molecular docking computations were carried out on a Dell Precision workstation with the RHEL X.0 operating system using Glide 5.6 (Schrodinger, L.L.C., New York, NY, U.S.A.).

Ligand Structure Preparation The molecular structures were first optimized using the Gaussian 03 software at the DFT/B3LYP/6-311G** level of theory. The optimization was verified by showing that the calculated vibrational frequencies were realistic.

Protein Structure Preparation The X-ray crystal structure of MtCYP51 in complex with the fluconazole (Flu) ligand (PDB ID: 1EA1) was obtained from the RCSB PDB and used to model the protein structure examined in the present study. The protein was optimized for docking using the "Protein Preparation Wizard" and "Prime-Refinement Utility" of Maestro 9.1 (Schrodinger, L.L.C.). The heme cofactor and the iron charges and connectivity were carefully inspected. A zero-order bond was present between the heme iron and the fluconazole ligand. This bond was broken prior to "picking" the ligand during the Glide grid generation.

Glide Docking The XP Glide docking method was used to dock compounds **6**, **7a**–**g**, and **8a**–**g** into the MtCYP51 binding site. The docking methodology is described I detail in the main text. The XP mode is a refinement tool designed for use only on good ligand conformations. The XP mode is less forgiving than the regular Glide mode, so it effectively screens out false positives. The XP mode is designed to identify active compounds that bind to a particular conformation of the receptor.[28]

Acknowledgments We thank M. E. Núñez Pastrana and P. Hernández-Morales from Facultad de Ciencias Químicas, CIEP, Universidad Autónoma de San Luis Potosí, for technical assistance. Financial support from FAI-UASLP Grants C10-FAI-05-16.43 and C10-FAI-05-14.41 are gratefully acknowledged. Thanks to CONACYT for a graduate fellowship 217383 for R. González-Chávez and we also thank R. O. Torres, E. Garcia, E. Bonilla, H. Rios, and J. Perez for technical assistance from the Instituto de Química, UNAM.

References and Notes

1) Amorim A., Guedes-Vaz L., Araujo R., *Int. J. Antimicrob. Agents*, **35**, 396–399 (2010).
2) Carlisle P. L., Banerjee M., Lazzell A., Monteagudo C., López-Ribot J. L., Kadosh D., *Proc. Natl. Acad. Sci. U.S.A.*, **106**, 599–604 (2009).
3) Prasad R., Gaur N. A., Gaur M., Komath S. S., *Infect. Disord. Drug Targets*, **6**, 69–83 (2006).
4) Ghannoum M. A., Rice L. B., *Clin. Microbiol. Rev.*, **12**, 501–517 (1999).
5) Kathiravan M. K., Salake A. B., Chothe A. S., Dudhe P. B., Watode R. P., Mukta M. S., Gadhwe S., *Bioorg. Med. Chem.*, **20**, 5678–5698 (2012).
6) Podust L. M., Poulos T. L., Waterman M. R., *Proc. Natl. Acad. Sci. U.S.A.*, **98**, 3068–3073 (2001).
7) Jia N., Arthington-Skaggs B., Lee W., Pierson C. A., Lees N. D., Eckstein J., Barbuch R., Bard M., *Antimicrob. Agents Chemother.*, **46**, 947–957 (2002).
8) Lepesheva G. I., Hargrove T. Y., Kleshchenko Y., Nes W. D., Villalta F., Waterman M. R., *Lipids*, **43**, 1117–1125 (2008).
9) Sheng C., Zhang W., Ji H., Zhang M., Song Y., Xu H., Zhu J., Miao Z., Jiang Q., Yao J., Zhou Y., Zhu J., Lü J., *J. Med. Chem.*, **49**, 2512–2525 (2006).
10) Neves M. A., Dinis T. C., Colombo G., Sá e Melo M. L., *J. Med. Chem.*, **52**, 143–150 (2009).
11) Slama J. T., Hancock J. L., Rho T., Sambucetti L., Bachmann K. A., *Biochem. Pharmacol.*, **55**, 1881–1892 (1998).
12) Sheehan D. J., Hitchcock C. A., Sibley C. M., *Clin. Microbiol. Rev.*, **12**, 40–79 (1999).
13) Ji H., Zhang W., Zhang M., Kudo M., Aoyama Y., Yoshida Y., Sheng C., Song Y., Yang S., Zhou Y., Lü J., Zhu J., *J. Med. Chem.*, **46**, 474–485 (2003).
14) Yao B., Ji H., Cao Y., Zhou Y., Zhu J., Lü J., Li Y., Chen J., Zheng C., Jiang Y., Liang R., Tang H., *J. Med. Chem.*, **50**, 5293–5300 (2007).
15) Babu K. S., Li X. C., Jacob M. R., Zhang Q., Khan S. I., Ferreira D., Clark A. M., *J. Med. Chem.*, **49**, 7877–7886 (2006).
16) Nes W. D., *Chem. Rev.*, **111**, 6423–6451 (2011).
17) Rossello A., Bertini S., Lapucci A., Macchia M., Martinelli A., Rapposelli S., Herreros E., Macchia B., *J. Med. Chem.*, **45**, 4903–4912 (2002).
18) Martínez R., Clara-Sosa A., Ramírez-Apan M. T., *Bioorg. Med. Chem.*, **15**, 3912–3918 (2007).
19) de la Fuente M., del Mar Fernández M., Zafra C., Solana R., Peña J., *Methods Find. Exp. Clin. Pharmacol.*, **6**, 241–243 (1984).
20) Chiang C. C., Lin Y. H., Lin S. F., Lai C. L., Liu C., Wei W. Y., Yang S. C., Wang R. W., Teng L. W., Chuang S. H., Chang J. M., Yuan T. T., Lee Y. S., Chen P., Chi W. K., Yang J. Y., Huang H. J., Liao C. B., Huang J. J., *J. Med. Chem.*, **53**, 5929–5941 (2010).
21) Vanotti E., Amici R., Bargiotti A., Berthelsen J., Bosotti R., Ciavolella A., Cirla A., Cristiani C., D'Alessio R., Forte B., Isacchi A., Martina K., Menichincheri M., Molinari A., Montagnoli A., Orsini P., Pillan A., Roletto F., Scolaro A., Tibolla M., Valsasina B., Varasi M., Volpi D., Santocanale C., *J. Med. Chem.*, **51**, 487–501 (2008).
22) Huang K. H., Veal J. M., Fadden R. P., Rice J. W., Eaves J., Strachan J. P., Barabasz A. F., Foley B. E., Barta T. E., Ma W., Silinski M. A., Hu M., Partridge J. M., Scott A., DuBois L. G., Freed T., Steed P. M., Ommen A. J., Smith E. D., Hughes P. F., Woodward A. R., Hanson G. J., McCall W. S., Markworth C. J., Hinkley L., Jenks M., Geng L., Lewis M., Otto J., Pronk B., Verleysen K., Hall S. E., *J. Med. Chem.*, **52**, 4288–4305 (2009).
23) Sheng C., Zhang W., Ji H., Zhang M., Song Y., Xu H., Zhu J., Miao Z., Jiang Q., Yao J., Zhou Y., Zhu J., Lü J., *J. Med. Chem.*, **49**, 2512–2525 (2006).
24) Podust L. M., Poulos T. L., Waterman M. R., *Proc. Natl. Acad. Sci. U.S.A.*, **98**, 3068–3073 (2001).
25) Podust L. M., Stojan J., Poulos T. L., Waterman M. R., *J. Inorg. Biochem.*, **87**, 227–235 (2001).
26) Patel P. D., Patel M. R., Kocsis B., Kocsis E., Graham S. M., Warren A. R., Nicholson S. M., Billack B., Fronczek F. R., Talele T. T., *Eur. J. Med. Chem.*, **45**, 2214–2222 (2010).
27) Xiao L., Madison V., Chau A. S., Loebenberg D., Palermo R. E., McNicholas P. M., *Antimicrob. Agents Chemother.*, **48**, 568–574 (2004).
28) Glide, version 5.6, Schrödinger, LLC, New York, NY, 2010.
29) Kellenberger E., Rodrigo J., Muller P., Rognan D., *Proteins*, **57**, 225–242 (2004).
30) Frisch M. J., Trucks G. W., Schlegel H. B., Scuseria G. E., Robb M. A., Cheeseman J. R., Montgomery J. A., Vreven T., Kudinb K. N., Burant J. C., Millam J. M., Iyengar S. S., Tomasi J., Barone V., Mennucci B., Cossi M., Scalmani G., Rega N., Pebterbsson G. A., Nakatsuji H., Hada M., Ehara M., Toyota K., Ukuda R., Hasegawa J., Ishida M., Nakajima T., Honda Y., Kitao O., Nakai H., Klene M., Li X., Knox J. E., Hratchian H. P., Cross J. B., Adamo C., Jaramillo J., Gomperts R., Stratmann R. E., Yazyev O., Austin A. J., Cammi R., Pomelli C., Ochterski J. W., Ayala P. Y., Morokuma K., Voth G. A., Salvador P., Dannenberg J. J., Zakrzewski V. G., Dapprich S., Daniels A. D., Strain M. C., Farkacs O., Malick D. K., Rabuck A. D., Raghavachari K., Foresman J. B., Ortiz J. V., Cui Q., Baboul A. G., Clifford S., Cioslowski J., Stefanov B. B., Liu G., Liashenko A., Piskorz P., Komaromi I., Martin R. L., Fox D. J., Keith T., Al-Laham M. A., Peng C. Y., Anayakkara A., Challacombe M., Gill P. M. W., Johnson B., Chen W., Wong M. W., Gonzalez C., Pople J. A., Gaussian 03, 2003.
31) Martínez R., Avila Z. G., Reyes A. E., *Synth. Commun.*, **25**, 1071–1076 (1995).
32) "CLSI, (2008a) Reference method for broth dilution antifungal susceptibility testing of yeasts; approved standard-third edition; CLSI document M27-A3," Clinical and Laboratory Standards Institute, Wayne.
33) "CLSI, (2008b) Reference method for broth dilution antifungal susceptibility testing of filamentous fungi; approved standard CLSI document M38-A2," Clinical and Laboratory Standards Institute, Wayne.